



Spatial distributions of the REFLEX-DXL galaxy clusters at $z \sim 0.3$ observed by XMM-Newton ^{*}

Y.-Y. Zhang¹, A. Finoguenov¹, H. Böhringer¹, Y. Ikebe^{1,2}, K. Matsushita^{1,3}, P. Schuecker¹, L. Guzzo⁴ and C. A. Collins⁵

¹ Max-Planck-Institut für extraterrestrische Physik, Garching, Germany;

² Joint Center for Astrophysics, University of Maryland, Baltimore, USA;

³ Tokyo University of Science, Tokyo, Japan;

⁴ INAF - Osservatorio Astronomico di Brera, Merate/Milano, Italy;

⁵ Liverpool John Moores University, Liverpool, U.K.

Abstract. We present XMM-Newton results on the spatially resolved temperature profiles of eight massive galaxy clusters of a volume-limited sample at redshifts $z \sim 0.3$ (REFLEX-DXL sample) and an additional luminous cluster at $z = 0.2578$, selected from the REFLEX survey. Useful temperature measurements could be performed out to radii with overdensity 500 (r_{500}). The scaled temperature distributions show good similarities. We discovered diversities in the temperature gradients at the outer cluster radii with examples of both flat and strongly decreasing profiles which call for different physical interpretations. We found an indication of the 'warm-hot' gas existing in or around the hot clusters. Using RXCJ0307.0–2840 we demonstrate that the errors on the mass estimates are within 25% up to r_{500} .

Key words. cosmology: observations – galaxies: clusters: general – X-rays: galaxies: clusters

1. Introduction

The most massive clusters are especially important in tracing large scale structure (LSS) evolution since they are expected to show the largest evolutionary effects. In hierarchical modeling the structure of

Send offprint requests to: Y.-Y. Zhang,
email: yyzhang@mpe.mpg.de

* This work is based on observations made with the XMM-Newton, an ESA science mission with instruments and contributions directly funded by ESA member states and the USA (NASA).

the X-ray emitting plasma in the most massive clusters is essentially determined by gravitational effects and shock heating. With decreasing cluster mass and intra-cluster medium (ICM) temperature, non-gravitational effects play an important role before and after the shock heating (Voit & Bryan 2001; Voit et al. 2002; Zhang & Wu 2003; Ponman et al. 2003). Therefore, the most massive clusters provide the cleanest results in comparing theory with observations.

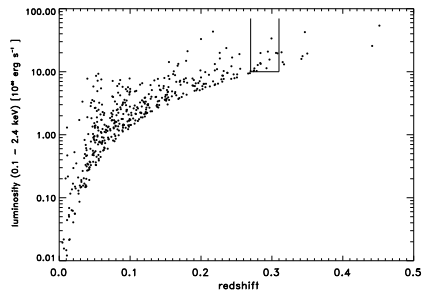


Fig. 1. X-ray luminosity-redshift distribution of the REFLEX clusters. The box shows the selection of the 13 REFLEX-DXL clusters (see Böhringer et al. 2003).

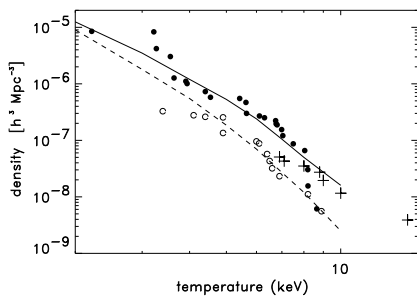


Fig. 2. A preliminary REFLEX-DXL temperature function (crosses) is compared to the $\langle z \rangle = 0.05$ (solid circles) and $\langle z \rangle = 0.38$ (open circles) temperature functions from Henry (2000). See Böhringer et al. 2003.

In this project we are analysing an almost volume-complete sample of thirteen X-ray luminous ($L_X \geq 10^{45} \text{ erg s}^{-1}$ for 0.1–2.4 keV) clusters selected from the ROSAT-ESO Flux-Limited X-ray (REFLEX) galaxy cluster survey (Böhringer et al. 2001) in the redshift interval $z = 0.27$ to 0.31 (see Fig. 1). There is only a very small correction to the volume completeness with a well known selection function for $L_X \geq 10^{45} \text{ erg s}^{-1}$ at the higher redshift as described in Böhringer et al. (2003). With this REFLEX-DXL (Distant X-ray Luminous) sample, we obtain reliable ICM tempera-

tures to measure the cluster masses based on the high resolution observations from XMM-Newton (Zhang et al 2004). Since peculiarities in the cluster structure introduce a scatter in the mass-temperature relation and since in particular on-going cluster mergers can lead to a temporary increase in the cluster temperature and X-ray luminosity (Randall et al. 2002), we aim for a detailed study of the deep XMM-Newton observations described here. The clusters are also scheduled for a detailed spectroscopic study of the cluster dynamics with the ESO-VLT-VIMOS instrument. One prime goal is to study the temperature function evolution (see Fig. 2, Böhringer et al. 2003) by comparing our sample with more nearby and more distant clusters in literature. The selection of the REFLEX-DXL sample and its properties are described in detail in Böhringer et al. (2003). The method is well described in Zhang et al. (2004), which is established for a reliable determination of the spatially resolved temperature profiles for the REFLEX-DXL clusters. XMM-Newton with its superior sensitivity combined with its good spatial resolution provides the best means for such studies (Arnaud et al. 2002). Previously, large data sets on cluster temperature profiles have been compiled from ASCA (e.g. Markevitch et al. 1998; White 2000; Finoguenov et al. 2001a; Finoguenov et al. 2002; Sanderson et al. 2003) and BeppoSAX observations (Molendi & De Grandi 1999; Ettori et al. 2002).

In this proceeding we contribute the temperature profile measurements, discuss physics of diversity, describe an indication for soft excess from warm InterGalactic Medium (IGM), and present the mass estimates. We adopt a flat Λ CDM cosmology with the density parameter $\Omega_m = 0.3$ and the Hubble constant $H_0 = 70 \text{ km s}^{-1} \text{ Mpc}^{-1}$. Error bars correspond to the 68% confidence level, unless explicitly stated otherwise.

2. Temperature distributions

We developed a reliable double background subtraction method for the XMM-Newton data reduction, in which we use the XMM-Newton observations of the Chandra Deep Field South (CDFS) background and model the difference of the target and CDFS backgrounds with the data from the outer Field of view (FOV). The details are available in Zhang et al (2004).

Comparing the spectral results, we have noted that the differences between the global temperatures of the regions covering radii of $0.5 < r < 4'$ and $r < 8'$, respectively, are caused by systematic differences in the temperature gradients. For a more detailed study of the temperature profiles we divide the cluster regions into the five annuli $0-0.5'$, $0.5-1'$, $1-2'$, $2-4'$, and $4-8'$.

We use > 1 keV band except for RXCJ0658.5–5556. We apply the 2–12 keV band for this high temperature cluster. The temperature profile of each cluster is shown in Zhang et al. (2004). We detect the gradients in the spatially resolved temperature profiles with an accuracy of better than 10 to 20% in the $r < 4'$ region. The temperatures vary as a function of the radius by a factor of 1.5 to 2. To some degree the difference of the central structure might reveal the effect of non-gravitational processes and radiative cooling. No significant cooling gas lower than 2 keV is found in the center.

In Fig. 3, we present the scaled temperatures of eight REFLEX-DXL clusters together with an additional cluster at slightly lower redshift $z = 0.2578$. The radii are scaled by the virial radii obtained from the M-T relation in Bryan and Norman (1998). The temperatures are scaled by the temperatures of the regions covering radii of $0.5 < r < 4'$, which cover almost the whole X-ray emission regions of the clusters. The grey shadow shows the self-similar temperature profile of Markevitch et al. (1998). The temperature profiles are on average flattened and the high accuracy of our data shows that the decrease in our temperature

profiles happens at further out radii. There are also diversities in the temperature profiles which were not observed before.

3. Physical interpretations

The variations of the temperature profiles call for different physical interpretations rather than simple reflections of measurement errors (see Fig. 4). Symmetric X-ray 2-D maps and regular temperature profiles suggest a relaxed dynamical state, e.g. RXCJ0307.0–2840. On the other hand irregular temperature profiles like diversities in the temperature gradients, e.g. RXCJ0658.5–5556, suggest mergers and/or significant substructures in those particular regions. Detailed spectroscopy of the particular regions should be performed based on the combination of the temperature profile and 2-D map implications. Since deprojection dilutes the fluctuations in 2-D maps, some clusters have regular temperature profiles but very disturbed structures in their 2-D maps, e.g. RXCJ1131.9–1955. Chandra and VLT observation are granted to study these interesting examples via their galaxy dynamics.

4. Soft excess

We found some inconsistencies in the fitting of the spectra with one temperature model, depending on the inclusion or exclusion of the 0.4–1 keV band, which could be an indication of the presence of a colder component. Cluster RXCJ1131.9–1955 is not affected at all, RXCJ0014.3–3022, RXCJ0307.0–2840 and RXCJ0528.9–3927 (see Fig. 5) are affected in the center, while RXCJ0043.4–2037 and RXCJ0232.2–4420 are affected in the outskirts. Since the instrumental setup used to observe this sample is the same, it hardly is an instrumental artifact. We notice that the temperature of RXCJ0528.9–3927 (also in other clusters) changes significantly with the low cut-off of the energy band used in the fit. We thus performed the X-ray spectral analysis to

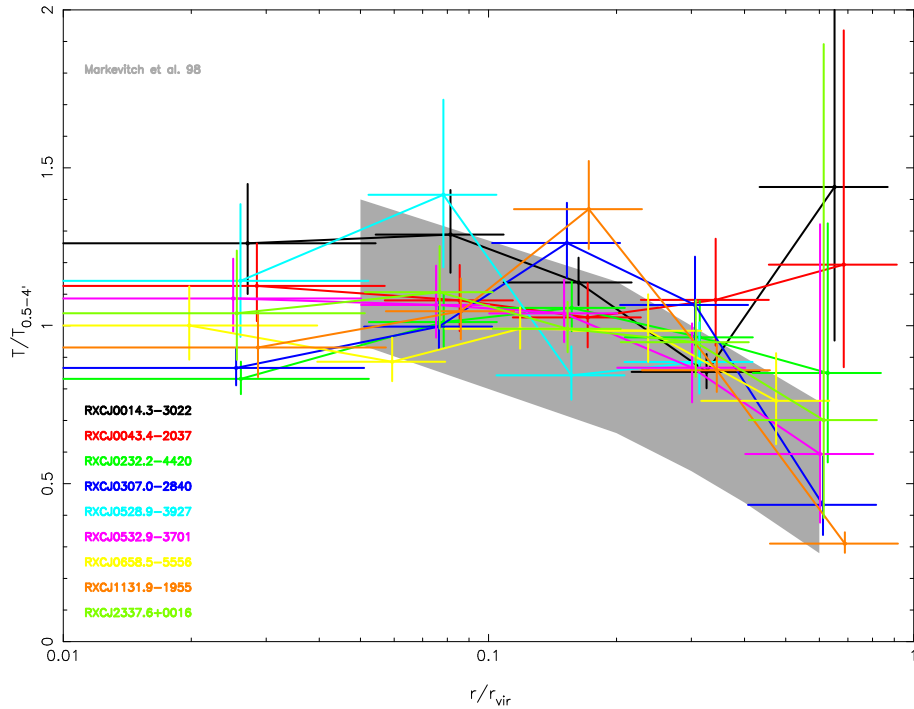


Fig. 3. Scaled temperature profiles fitted in the 1–10 keV band, noted the temperature profile of RXCJ0658.5–5556 was fitted in the 2–12 keV band.

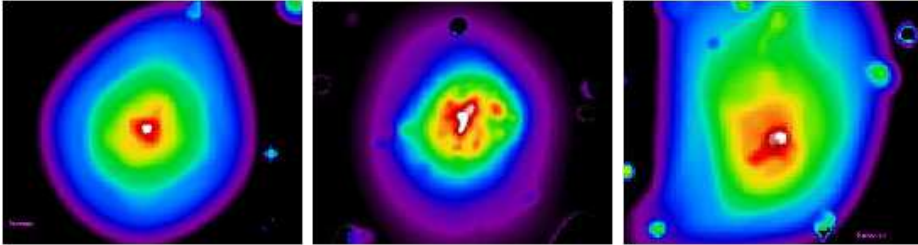


Fig. 4. Pressure maps of RXCJ0307.0–2840 (left), RXCJ0658.5–5556 (middle) and RXCJ1131.9–1955 (right).

test the energy band dependence and possible method dependence by comparing the temperature measurements versus low energy band (low-E) cut-off from two different methods: the double background subtraction method in Zhang et al. (2004) and the method applied in Arnaud et al. (2002). We found that soft excess exists independent of the method.

The metallicity and redshift measurements among the different methods and different low-E cut-off vary within 5%. The results presented in Fig. 5 suggest some influence of the low energy band on the temperature measurements. Thus the global galaxy cluster temperature is underestimated including the soft band. The results obtained in the harder energy band should recover the correct cluster temper-

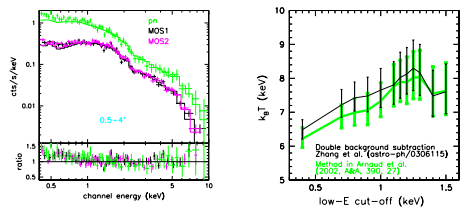


Fig. 5. Left: Spectra of RXCJ0528.9–3927 fitted in the 1–10 keV band. Right: Temperature measurements versus low-E cut-off.

ature. Similar phenomena are found for A1413 (Pratt & Arnaud 2002) using XMM-Newton data, and Coma, A1795 and A3112 (Nevalainen et al. 2003) based on the comparison of XMM-Newton and ROSAT PSPC observations. Nevalainen et al. interpret it as a ‘warm-hot’ intergalactic medium. The ‘warm-hot’ gas existing in or around the hot clusters might be related with the LSS environment.

5. Modeling RXCJ0307.0–2840

We use RXCJ0307.0–2840 as an illustrative example to demonstrate the accuracy of measurements of the total gravitating cluster mass and the gas mass fraction attainable with the XMM-Newton observations of the REFLEX-DXL-like clusters. Similar analysis of all REFLEX-DXL clusters is in progress.

According to the regularity of the photon distribution of RXCJ0307.0–2840 (see Fig. 4) we assume a radially symmetric gas distribution. We found that the parameterization

$$k_B T(r) = \frac{1}{Ar^2 + Br + C} \quad (1)$$

fits the measured temperature profiles quite well. The polytropic index (~ 1.59) of the temperature distribution in the outskirts implies a convectively stable state there. For the electron density distribution we use the standard β model (Michie 1961). Navarro et al. (1997; NFW) described a

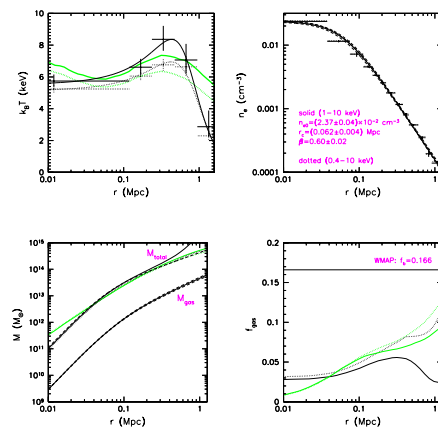


Fig. 6. Spatial distributions of the temperature (top left), electron density (top right), gas mass and gravitational mass (bottom left), and gas mass fraction (bottom right) for RXCJ0307.0–2840 using Method I (black) and Method II (green). An additional dashed curve of the gravitational mass presents the result of the isothermal β model.

universal density profile for dark matter (DM) from numerical simulations in hierarchical clustering scenarios. We assume the intracluster gas to be in hydrostatic equilibrium with the underlying gravitational potential dominated by DM component.

We thus demonstrate two methods to obtain the modeling of the spatial distributions of RXCJ0307.0–2840. One is to combine the β model, Eq.(1) and hydrostatic equilibrium (here after Method I); the other is to combine the β model, NFW model and hydrostatic equilibrium (here after Method II). In Fig 6, we present the spatially resolved temperature, electron number density, total mass, gas mass, and gas mass fraction distributions of RXCJ0307.0–2840. The uncertainties in the mass estimates are within 25 percent based on our temperature measurements. We found a slightly lower gas mass fraction comparing the WMAP result.

6. Summary and Conclusions

We obtain spatially resolved, consistent X-ray temperature profiles from three instruments for 9 clusters with an accuracy of better than 10–20% in the $< 4'$ region. We found good similarities in the scaled temperature distributions. While the high accuracy of our data shows that the decrease in our data happens at further out radii comparing to the self-similar temperature profile of Markevitch et al. (1998). Temperature structures are easily disturbed by some physical processes and are thus complicated. Differences of the central structures reveal the effect of non-gravitational process. No significant cooling gas (< 2 keV) is found in the center. The variations of the temperature distributions in the outer region call for different formation histories (e.g. Finoguenov et al 2001b). Among the sample, six clusters show regular temperature structures, while three do not. Combination of the regular temperature profiles and symmetric 2-D maps suggest a relaxed dynamical state. Fluctuations noted in 2-D maps might be diluted in the temperature profiles. The uncertainty in the temperature measurements is a key point to the accurate determinations of mass, gas mass fraction, and thus affects the L-T and M-T scaling relations.

Acknowledgements. The XMM-Newton project is supported by the Bundesministerium für Bildung und Forschung, Deutsches Zentrum für Luft und Raumfahrt (BMBF/DLR), the Max-Planck Society and the Haidenhaim-Stiftung. We acknowledge Jacqueline Bergeron, PI of the CDFS XMM-Newton observation, Martin Turner, PI of the RXJ0658.5-5556 XMM-Newton observation, Michael Freyberg, Ulrich G. Briel, and William R. Forman providing useful suggestions. YYZ acknowledges receiving the International Max-Planck Research School Fellowship. AF acknowledges receiving the Max-Planck-Gesellschaft Fellowship. PS acknowledges support under the DLR grant No. 50 OR 9708 35.

References

- Arnaud, M., Majerowicz, S., Lumb, D., et al. 2002, *A&A*, 390, 27
 Böhringer, H., Schuecker, P., Guzzo, L., et al. 2001, *A&A*, 369, 826
 Böhringer, H., Schuecker, P., Zhang, Y.-Y., et al. 2003, *A&A*, to be submitted.
 Bryan, G. L., & Norman, M. L. 1998, *ApJ*, 495, 80
 Ettori, S., De Grandi, S., & Molendi, S. 2002, *A&A*, 391, 841
 Finoguenov, A., Arnaud, M., & David, L. P. 2001a, *ApJ*, 555, 191
 Finoguenov, A., Reiprich, T. H., & Böhringer, H. 2001b, *A&A*, 368, 749
 Finoguenov, A., Jones, C., Böhringer, H., & Ponman, T. J. 2002, *ApJ*, 578, 74
 Henry, J. P. 2000, *ApJ*, 534, 565
 Markevitch, M., Forman, W. R., Sarazin, C. L., & Vikhlinin, A. 1998, *ApJ*, 503, 77
 Michie, R. W., 1961, *ApJ*, 133, 781
 Molendi, S., & De Grandi, S. 1999, *A&A*, 351, L41
 Navarro, J. F., Frenk, C. S., & White, S. D. M. 1997, *ApJ*, 490, 493 (NFW)
 Nevalainen, J., Lieu, R., Bonamente, M., & Lumb, D. 2003, *ApJ*, 584, 716
 Ponman, T. J., Sanderson, A. J. R., & Finoguenov, A. 2003, *MNRAS*, 343, 331
 Pratt, G. W., & Arnaud, M. 2002, *A&A*, 394, 375
 Randall, S. W., Sarazin, C. L., & Ricker, P. M. 2002, *AAS*, 201, 6706
 Sanderson, A. J. R., Ponman, T. J., Finoguenov, A., Lloyd-Davies, E. J., Markevitch, M. 2003, *MNRAS*, 340, 989
 Voit, G. M., & Bryan, G. L. 2001, *Nature*, 414, 425
 Voit, G. M., Bryan, G. L., Balogh, M. L., & Bower, R. G. 2002, *ApJ*, 576, 601
 White, D. A. 2000, *MNRAS*, 312, 663
 Zhang, Y.-Y., Finoguenov, A., Böhringer, H., et al. 2003, *A&A*, 413, 49
 Zhang, Y.-Y., & Wu, X.-P. 2003, *ApJ*, 583, 529